Sensors & Actuators: B. Chemical 348 (2021) 130540

Contents lists available at ScienceDirect

Sensors and Actuators: B. Chemical

journal homepage: www.elsevier.com/locate/snb

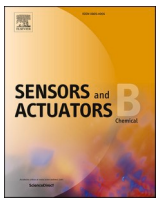

Development of Ag and Ag alloys-precipitated Ag_2O-TeO_2 glass and Ag_2O-TeO_2 glass/stainless steel reference electrodes for pH sensors

Tadanori Hashimoto [a,*], Keisuke Nakade [a], Atsushi Ishihara [a], Yuji Nishio [b]

[a] Division of Chemistry for Materials, Graduate School of Engineering, Mie University, 1577 Kurimamachiya-Cho, Tsu, Mie, 514-8507, Japan
[b] HORIBA Advanced Techno, Co., Ltd., 2 Miyanohigasi, Kisshoin, Minami-Ku, Kyoto, 601-8551, Japan

ARTICLE INFO

Keywords:
Ag
Ag alloy
Ag_2O-TeO_2 glass
Stainless steel
Reference electrode
pH sensor

ABSTRACT

An Ag/AgCl reference electrode that is built into commercially available pH electrodes leaks its internal KCl solution via a liquid junction. This leakage is disadvantageous because the test solution is contaminated by a trace amount of the KCl solution. The applicability of Ag_2O-TeO_2 glasses to reference electrodes for pH sensors was investigated in this study. The effects of the Ag_2O content and heat treatment on the pH sensitivity of these glasses and the pH sensitivity of the Ag_2O-TeO_2 glass/stainless steel electrodes were examined. The pH sensitivity of Ag_2O-TeO_2 glasses increased as the Ag_2O content increased, but it was less than 40 % and was the lowest among the glasses that have been investigated to date. The heat-treated $25Ag_2O{\cdot}75TeO_2$ glass and $25Ag_2O{\cdot}75TeO_2$ glass/stainless steel electrodes precipitated cubic Ag and hexagonal Ag and showed relatively low pH sensitivities of 26 % and 5 %, respectively. Thus, the hexagonal Ag and Ag alloys-precipitated samples were considered candidate reference electrodes for pH sensors.

1. Introduction

Commercially available pH combination electrodes often consist of two electrodes in principle: (1) a working electrode (lithium silicate-based glass) that generates an electromotive force in response to the concentration of hydrogen ions in the solution and (2) a reference electrode (Ag/AgCl). Lithium silicate-based glass electrodes show ideal Nernstian pH sensitivity that is independent of redox interference, a short pH response time, high repeatability, and a long lifetime along with high chemical durability over a wide pH range. However, the pH sensitivity decreases, and the pH response time increases as contamination accumulates during the continuous operation of the responsive glass membrane and liquid junction. For this reason, we have developed pH glass electrodes such as (1) TiO_2-coated commercially available pH-responsive glass electrodes [1] and titanophosphate glasses [2] with a self-cleaning property that is based on the photocatalytic activity and photoinduced hydrophilicity and iron-bismuthate glasses with an anti-fouling property that is based on their hydrophobicity [3–5]. We have also developed disposable stainless steel pH electrodes for which dirt is not a concern [6,7].

Glass sensors are unsuitable for in vivo biomedical, clinical, or food applications due to the brittleness of glass and the difficulty in measuring small volumes [8]. Therefore, low-cost electrodes [9–11], all-solid-state pH electrodes [12–16], disposable pH electrodes [17–19] and wearable pH electrodes [15,20,21] have been developed. However, an Ag/AgCl reference electrode that is built into commercially available pH electrodes leaks its internal KCl solution via a liquid junction to electrically contact Ag/AgCl and the test solution. This is disadvantageous because the test solution becomes contaminated by a trace amount of the KCl solution. This is a major problem in the food industry and biotechnology, although this is avoided by the use of a working electrode with an electrolyte bridge. Furthermore, there are numerous other shortcomings in the use of electrochemical electrodes with liquid system components, such as the limits of their miniaturization, positional dependencies during storage and use, limitations in use at high and low pressures and temperatures. Various solid-state reference electrodes have been developed, which are classified as Ag/AgCl electrodes [22–26], other electrodes [13,27–30] and reference-less electrodes [31–33]. The consumed KCl solution cannot be supplied again, and the pH electrode cannot be reused because polymers that are

Keywords: 25Ag75Te/SUS, $25Ag_2O{\cdot}75TeO_2$ glass/stainless steel enamel; xAg(100-x)Te, $x{Ag_2O}{\cdot}(100\text{-}x){TeO_2}$; bcc, body centered cubic; CTE, coefficient of thermal expansion; fcc, face centered cubic; DTA, differential thermal analysis; T_g, glass transition temperature; T_p, crystallization peak temperature; T_m, melting temperature; XRD, X-ray diffraction.

* Corresponding author.
E-mail address: hasimoto@chem.mie-u.ac.jp (T. Hashimoto).

https://doi.org/10.1016/j.snb.2021.130540
Received 30 March 2021; Received in revised form 25 July 2021; Accepted 29 July 2021
Available online 2 August 2021

immersed in the KCl solution are used in many Ag/AgCl electrodes.

We have reported that Fe_2O_3-Bi_2O_3 glasses have very low pH sensitivity and are candidate reference electrodes for pH sensors [3–5]. However, the resistivity of the glasses was too high for amplifiers that were equipped with a general pH meter and had incorrectly low pH sensitivity. We attempted to develop another candidate Ag_2O-containing glass for reference electrodes for pH sensors because Ag/AgCl is used as a commercially available reference electrode. Tellurite glasses [34,35] and phosphate glasses [36,37] can have relatively high Ag_2O contents. It is well known that the thermochemical reduction from Ag^+ ions to Ag^0 atoms can be promoted by Te^{4+} ions in the tellurite glass system [38]. Therefore, the effect of Ag precipitation on pH sensitivity is very interesting.

Glass electrodes have the disadvantage of being brittle, and metal electrodes have low chemical durability. Enamels with glass/metal structures [13,30,39,40] may resolve these problems. There are several requirements for enamel: (1) the glass must have the desired pH sensitivity (100 % for the working electrode and 0 % for the reference electrode), (2) the mismatch in the thermal expansion coefficients between the glass and the metal substrate must be small, and (3) fusion at a relatively low temperature must be easy [41,42]. We selected stainless steel SUS304 as a substrate for preparing enamel due to its ease of handling compared with carbon steel. For example, tellurite glasses [41,42] have coefficients of thermal expansion (CTE) of 12–18 $\times$ 10^{-6} K^{-1}, and this range is relatively close to the CTE of stainless steel 304, namely, 18 $\times$ 10^{-6} K^{-1} [43,44]. The applicability of Ag_2O-TeO_2 glasses to reference electrodes for pH sensors was investigated in the present study. The effects of Ag_2O content and heat treatment on the pH sensitivity of these glasses and the pH sensitivity of Ag_2O-TeO_2 glass/stainless steel electrodes were investigated.

2. Experimental

2.1. Glass preparation

$x$$Ag_2O$·(100-$x$)$TeO_2$ (xAg(100-x)Te, x = 15–30 mol%) glasses were produced via a conventional melt-quenching method. The following reagents were used as received: Ag_2O (99 % up, Kojundo Chemical Lab. Co., Ltd., Sakado, Japan) and TeO_2 (99.9 %, Kojundo Chemical Lab. Co., Ltd., Sakado, Japan). Batches (20 or 30 g) in alumina crucibles with caps were directly heated at 900 ℃ for 1 h without mixing the melts. The obtained melts were pressed by stainless steel that was heated at 200 ℃ and annealed at 200 ℃ for 1 h. 25Ag_2O·75TeO_2 glass was abbreviated as 25Ag75Te. xAg(100-x)Te glass was polished for pH and electrical resistivity measurements.

2.2. Heat treatment of glass

Heat-treated 25Ag75Te was obtained by heat-treating 25Ag75Te plate glass at 250 or 275 ℃ for 24 h under an air atmosphere after optically polishing the plate glass. The 25Ag75Te glass/stainless steel enamel was prepared as follows because handling samples that were heat-treated at higher temperatures was difficult. The 25Ag75Te glass was crushed and classified as 25Ag75Te glass powder of less than 53 μm. The 25Ag75Te glass powder was deposited on stainless steel SUS304 (Nilaco Corporation, Tokyo, Japan) with a thickness of 0.2 mm using the dry-type doctor blade method. Then, 25Ag75Te glass/stainless steel enamel (abbreviated 25Ag75Te/SUS) was obtained via heat treatment at 640 or 680 ℃ for 2.0 h under an N_2 atmosphere to fuse the 25Ag75Te glass powder onto the stainless steel. The stainless steel serves as a back electrode that supports the 25Ag75Te glass at high heat treatment temperatures because the stainless steel does not contact the test solution in potentiometric measurements.

2.3. Potentiometric measurement of samples

Potentiometric measurements for the xAg(100-x)Te glasses, heat-treated 25Ag75Te glasses, and 25Ag75Te/SUS were conducted for a handmade polyvinyl chloride (PVC) cell with a sample plate with dimensions of 16 mm $\times$ 16 mm $\times$~1 mm at 25 ℃ (Fig. 1). The cell contained an Ag/AgCl electrode as an internal electrode and a KCl buffer solution as an internal solution. The time intervals that were used with an F-72 or F-74 pH meter (HORIBA, Ltd., Kyoto, Japan) and a portable ZR-RX20 multilogger (OMRON Corp., Kyoto, Japan) were 3 s and 0.5 s, respectively. Electrode 2565 (HORIBA, Ltd., Kyoto, Japan), which consists of an Ag/AgCl, 3.33 mol/L Cl^- electrode as an internal electrode, and a KCl aqueous solution as an internal solution, was used as a reference electrode. The pH sensitivity is described in detail in Refs. [2–7]. Potentiometric measurement of three cycles was conducted in the order of pH 6.86 (150-7, monopotassium phosphate and disodium phosphate, HORIBA, Ltd., Kyoto, Japan, abbreviated as pH 7), pH 4.01 (150-4, potassium hydrogen phthalate, HORIBA, Ltd., Kyoto, Japan, abbreviated as pH 4) and pH 9.18 (150-9, sodium borate, HORIBA, Ltd., Kyoto, Japan, abbreviated as pH 9) according to JIS Z 8805. Potentials after 3 min in the third cycle at pH 7, pH 4, and pH 9 were determined to be stable in all potentiometric measurements.

In this case (25 ℃), the potential decreases ideally by 59.16 mV/pH with increasing pH according to the Nernst equation. The pH responsivity (pH sensitivity, pH repeatability, and pH response time) was determined as follows. Then, the pH a–b sensitivity between pH a and pH b was estimated from potentials E_a and E_b via Eq. (1).

$$\text{pH a–b sensitivity } (\%) = -100F(E_a\text{-}E_b)/2.3026RT(\text{pH a-pH b}) \quad (1)$$

where E_a, E_b, R, T, and F are the potentials of the working electrode versus the reference electrode at pH a and pH b, the gas constant (8.3145 J/K mol), the absolute temperature, and the Faraday constant (96485 C/mol), respectively. In addition, the pH repeatability was defined as the maximum difference in the potential after 3 min at pH 7 for three cycles. The pH response time was defined as the average time that was required to reach a constant potential with fluctuations of less than ±0.5 mV/s for pH 4, 7, and 9 measured at time intervals of 3 s using a pH meter.

2.4. Characterization of samples

The DC electrical resistivities of the 25Ag75Te glass and 25Ag75Te/SUS with ~1 mm thickness and an Ag electrode of 6 mm ϕ on both sides were measured at 25 ℃ using an SM-8215 super megohm meter (HIOKI E. E. Corp., Ueda, Japan). The electrical resistivity of ion conductive glass should be measured under AC conditions [36,37]. In the present study, simple DC measurements were conducted to screen samples with high electrical resistivity because the results under AC and DC of 25Ag75Te glass were 5.2·10^8 Ω cm and 6.0·10^8 Ω cm, respectively. Differential thermal analysis (DTA) measurements of xAg(100-x)Te

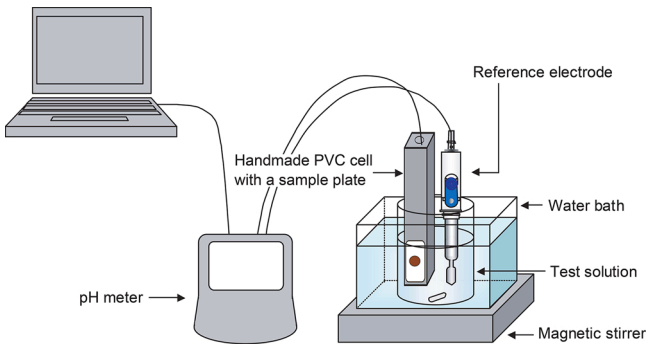

Fig. 1. Apparatus for potentiometric measurement using handmade PVC cell with a sample plate versus a commercially available reference electrode.

glasses using DTG-60AH (Shimadzu Corp., Kyoto, Japan) were performed under air. The following conditions were used: a flow rate of 100 ml/min, a temperature of 1000 ℃ at a heating rate of 10 ℃/min, without retention at the target temperature, and furnace cooling. X-ray diffraction (XRD) patterns of the crystalline phases that precipitated in the 25Ag75Te glass, heat-treated 25Ag75Te glasses, and 25Ag75Te/SUS were measured using an Ultima IV XRD measurement system (Rigaku Corp., Tokyo, Japan). The following conditions were used: X-ray source Ni-filtered Cu-Kα radiation (λ = 0.15405 nm), 2θ = 30–50 °, a sampling width of 0.02 °, a scan speed of 1 °/min, a voltage of 40 kV, a current of 40 mA, a radiation slit of 2/3 °, a radiation column limitation slit of 10.00 mm, a scattering slit of 0.05 mm, a detection slit of 0.45 mm, an offset angle of 0 ° and an accumulation number of 4.

In addition, the influence of interfering ions (Na^+ and Cl^-) on the potential of 25Ag75Te/SUS (680 ℃-2.0 h) was investigated using Na^+-free pH 4 buffer solutions (150-4) adding NaCl (99.5 %, guaranteed reagent grade, Nacalai Tesque, Inc., Kyoto, Japan) of 1.71×10^{-2}–$1.71 \times$ 10 mmol/L corresponding to 0.001–1 g/L. The potential after 3 min was used as a stable one in all potentiometric measurements.

3. Results and discussion

3.1. Appearance and thermal properties of xAg(100-x)Te glasses

Fig. 2 shows photographs of *x*Ag(100-*x*)Te glasses and 25Ag75Te/SUS (680 ℃-2.0 h). The color of *x*Ag(100-*x*)Te glasses changed from yellow to dark red with increasing Ag_2O content. 25Ag75Te/SUS (680 ℃-2.0 h) had a brown rugged surface, which suggests that the glass matrix was partially crystallized. The results of the DTA measurement of *x*Ag(100-*x*)Te glasses are summarized in Table 1. The glass transition temperature (T_g), crystallization peak temperature (T_p), and melting temperature (T_m) decreased with increasing Ag_2O content. T_p-T_g increased with increasing Ag_2O content; hence, the thermal stability of the glasses increased.

3.2. pH response of xAg(100-x)Te glasses

Fig. 3 presents the changes in potential with the measurement time for 25Ag75Te glass and 20Fe60Bi20Ge [5] in pH 7, pH 4, and pH 9 buffer solutions. The change in potential with the measurement time that corresponds to a pH change is large for 20Fe60Bi20Ge, which suggests that it serves as a working electrode. In contrast, that of 25Ag75Te glass is relatively small, which suggests that it serves as a reference electrode. The pH responsivity (pH sensitivity, pH repeatability, and pH response time) and electrical resistivity results for

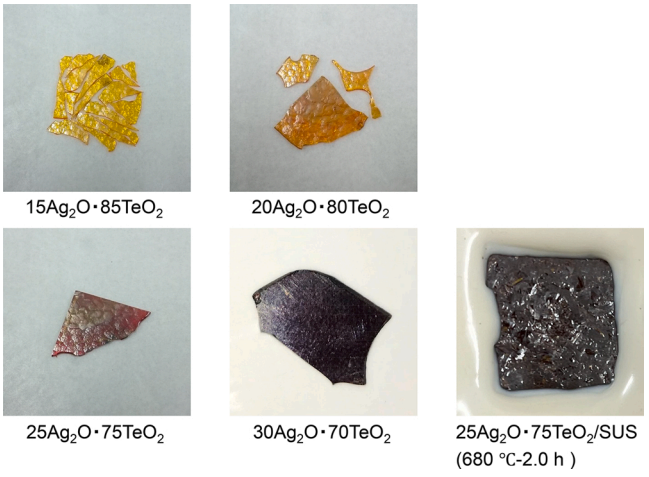

Fig. 2. Photographs of *x*Ag(100-*x*)Te glasses and 25Ag75Te/SUS (680 ℃–2.0 h).

Table 1
Glass transition temperature (T_g), crystallization peak temperature (T_p), T_p-T_g, and melting temperature (T_m) of *x*Ag(100-*x*)Te glasses.

Sample Name	T_g (℃)	T_p (℃)	T_p-T_g (℃)	T_m (℃)
15Ag85Te	311	424	113	546
20Ag80Te	288	396	108	481
25Ag75Te	247	380	133	487
30Ag70Te	214	373	159	485

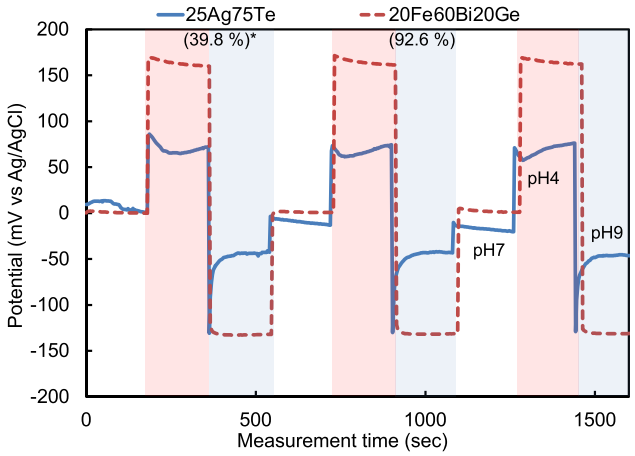

*: pH sensitivity between pH 4-9

Fig. 3. Changes in potential with the measurement time for 25Ag75Te glass and 20Fe60Bi20Ge glass [5] in pH 7, pH 4, and pH 9 buffer solutions.

25Ag75Te glasses and related samples are listed in Table 2. Under "pH sensitivity", the column entitled pH 4–9 presents the sensitivity between pH 4 and pH 9. The sensitivity between pH 7 and pH 9 of 25Ag75Te was lower than that between pH 4 and pH 7 (Table 2).

Fig. 4 presents the relationship between the pH sensitivity and electrical resistivity of *x*Ag(100-*x*)Te glasses. The dotted area indicates the electrical resistivity region above 2×10^{10} Ω cm, in which the pH sensitivity is less reliable. The region arises from the restriction of the amplifier of the pH meter and was empirically determined based on the electrical resistivity of 1×10^{10} Ω cm for commercially available pH-responsive glass [2–4]. Thus, the low pH sensitivities of 15Ag85Te and 20Ag80Te, which tend to show noisy potential curves, may not be accurate. The pH sensitivities and the electrical resistivity of *x*Ag(100-*x*)Te glasses tend to increase and decrease with increasing Ag_2O content, respectively. However, the pH sensitivity below 40 % is the lowest among those of the glasses that have been investigated to date except glasses with high electrical resistivity [1–7]. *x*Ag(100-*x*)Te glasses were desirable as reference electrodes rather than working electrodes for pH sensors. We have focused on 25Ag75 glass with lower resistivity henceforth because Ag° precipitation on the glass surface during heat treatment decreases the concentration of internal Ag^+ ions and increases the electrical resistivity of the glass.

3.3. pH response of heat-treated 25Ag75Te glasses

Next, the effect of heat treatment of 25Ag75Te glasses on the pH sensitivity was investigated. Fig. 5 shows the changes in potential with the measurement time for 25Ag75Te and heat-treated 25Ag75Te glasses in pH 7, pH 4, and pH 9 buffer solutions. The pH sensitivity of heat-treated 25Ag75Te (250 ℃-24 h) was ~26 %, which was lower than that before heat treatment (~40 %). The pH sensitivity of heat-treated 25Ag75Te (275 ℃-24 h) showed values that were close to 25Ag75Te (250 ℃-24 h), as listed in Table 2. The values are close to a pH sensitivity

Table 2
pH responsivity (pH sensitivity, pH repeatability, and pH response time) and electrical resistivity of 25Ag75Te glasses and related samples.

Sample Name	pH Sensitivity (%)			pH Repeatability	pH Response Time	Electrical Resistivity
	pH 4–7	pH 7–9	pH 4–9	(pH)	(sec)	(Ω cm)
25Ag75Te	57.2	18.4	39.8	0.14	20	5.97×10^{8}
25Ag75Te (250 ℃–24 h)	37.0	12.7	26.1	0.15	13	N.M.[*1]
25Ag75Te (275 ℃–24 h)	36.3	16.9	27.6	0.41	17	N.M.
25Ag75Te/SUS (640 ℃–2.0 h)	47.0	0.9	26.3	0.28	17	2.71×10^{9}
25Ag75Te/SUS (680 ℃–2.0 h)	4.7	5.0	4.8	0.44	8	1.33×10^{9}
Ag	18.0	21.8	19.8	0.25	11	1.59×10^{-6}
SUS (600 ℃–24 h)	105.6	96.7	101.6	0.28	13	7.20×10^{-5}

[*] 1: N.M.: not measured.

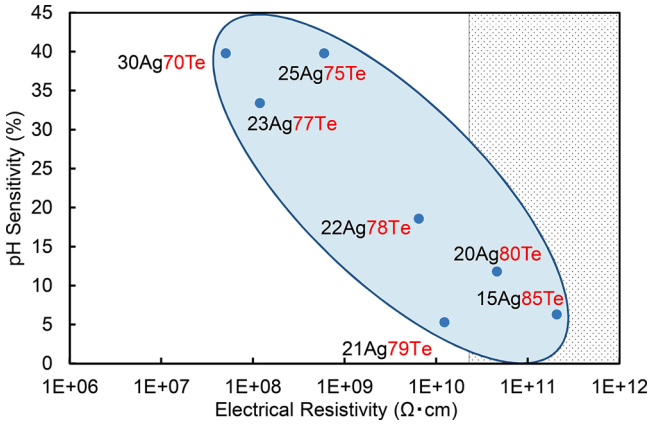

Fig. 4. Relationship between pH sensitivity and electrical resistivity of *x*Ag (100-*x*)Te glasses.

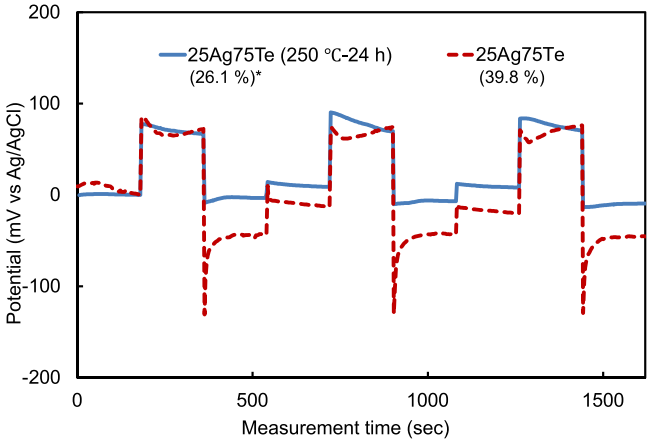

*: pH sensitivity between pH 4-9

Fig. 5. Changes in the potential with the measurement time for 25Ag75Te and heat-treated 25Ag75Te (250 ℃–24 h) glasses in pH 7, pH 4, and pH 9 buffer solutions.

of ~ 20 % for Ag. These results may be related to the precipitation of Ag from the glass because Ag° easily precipitates from Ag_2O-containing glasses [35–38]. When samples are heat-treated at higher temperatures, Ag precipitation is expected to accelerate and approach the pH sensitivity of Ag. 25Ag75Te glass/stainless steel enamel was prepared because handling samples that were heat-treated at higher temperatures was difficult.

3.4. pH response of heat-treated 25Ag75Te glasses/stainless steel enamel

Fig. 6 presents the changes in potential with the measurement time for 25Ag75Te and 25Ag75Te/SUS (680 ℃-2.0 h) in pH 7, pH 4, and pH 9 buffer solutions. 25Ag75Te/SUS (680 ℃-2.0 h) showed a much smaller change in potential than 25Ag75Te glass. 25Ag75Te/SUS (680 ℃-2.0 h) showed a very low pH sensitivity of ~5 %. The pH response time decreased because the change in the potential curve with pH became small. The pH sensitivity of 25Ag75Te/SUS is much lower than that of stainless steel with high pH sensitivity and close to that of 25Ag75Te glass. Low pH sensitivity of the glass surface is observed because the 25Ag75Te layer is a thick film and the pH sensitivity is low. In contrast, the pH sensitivity of SUS that was coated with a transition metal oxide thin film was close to that of SUS [6,7]. A slight drift of potential was observed for 25Ag75Te/SUS (680 ℃–2.0 h). It is reported that the stability of the potential of Ag is worse than Ag/AgCl [45]. Improvement of stability of potential due to chlorination is a plan.

Enamel pH electrodes with glass/metal structures are commercially available from Pfaudler, Inc., but it is very expensive [40]. The upper glass-lined layer (measuring electrode, “pH glass-lining”) reacts to hydrogen ions (H^{+}) and emits a concentration-dependent potential. The lower glass-lined layer (reference electrode, “reference glass-lining”) reacts to the salts dissolved in the fluid, in particular sodium ions, thus emitting a product-specific reference potential. The latter is considered to be so-called sodium-responsive glasses [46,47] and the potential changes by 59 mV/pNa with Na concentration. The influence of interfering ions (Na^{+} and Cl^{-}) on the potential of 25Ag75Te/SUS (680 ℃-2.0 h) was investigated (Fig. 7). The response changed by 8 mV/pNa between 1.71×10^{-2}–1.71 mmol/L corresponding to 0.001–0.1 g/L. The potential decreased at higher NaCl concentrations. 25Ag75Te/SUS (680 ℃–2.0 h) is superior to the above commercial enamel reference electrode at this point.

3.5. Effect of the crystal phase on the pH sensitivity

Interestingly, the pH sensitivity of 25Ag75Te/SUS (680 ℃–2.0 h) is much lower than that of Ag, as presented in Table 2. The crystal phase of Ag that precipitated in the samples was investigated via XRD. Fig. 8 shows the XRD patterns of 25Ag75Te glass, heat-treated 25Ag75Te glass, 25Ag75Te/SUS, and the reference Ag. The circles, triangles, and squares in this figure represent Ag (cubic Ag: JCPDS card No. 04-0783, hexagonal Ag: JCPDS card No. 41-1402), Ag alloys (Ag_2Te: JCPDS card No. 34-0142, $Ag_{1.85}Te$: JCPDS card No. 18-1186, Ag_7Te_4: JCPDS card No. 18-1187, and AgTe: JCPDS card No. 16-0412) and TeO_2 (α-TeO_2: JCPDS card No. 42-1365 and β-TeO_2: JCPDS card No. 07-0860), respectively. 25Ag75 glass, which had a pH sensitivity of ~40 %, was X-ray amorphous (Table 2). 25Ag75Te (250 ℃–24 h) precipitated cubic Ag along with α-TeO_2 and β-TeO_2. 25Ag75Te (250 ℃–24 h) and cubic Ag plate had a pH sensitivity of ~20 %. 25Ag75Te/SUS (640 ℃–2.0 h) precipitated hexagonal Ag, Ag_2Te, and $Ag_{1.85}Te$ along with α-TeO_2 and β-TeO_2. Ag is present as a cubic phase in nature, whereas hexagonal Ag is observed in nanosized Ag [48,49]. The pH sensitivity of 25Ag75Te/SUS

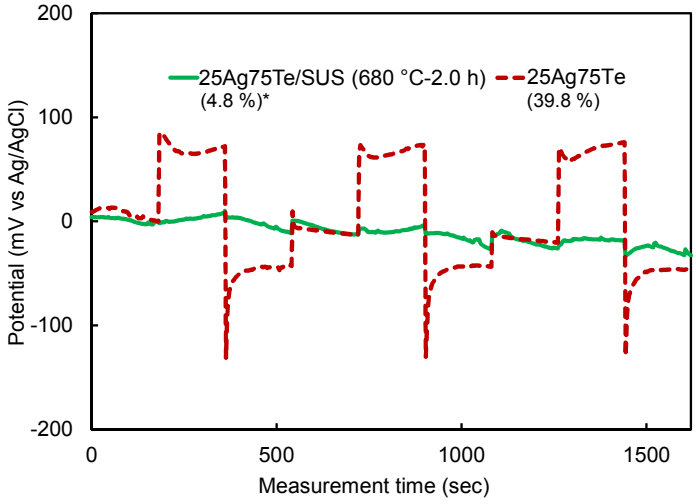

Fig. 6. Changes in potential with the measurement time for 25Ag75Te and 25Ag75Te/SUS (680 ℃-2.0 h) in pH 7, pH 4, and pH 9 buffer solutions.

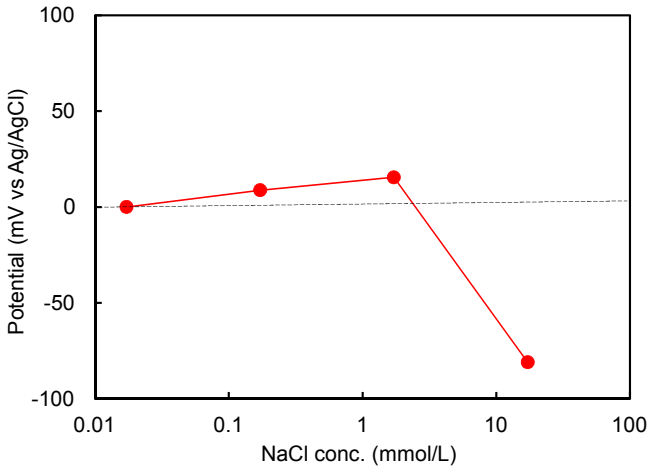

Fig. 7. Influence of interfering ions (Na^+ and Cl^-) on the potential of 25Ag75Te/SUS (680 ℃–2.0 h).

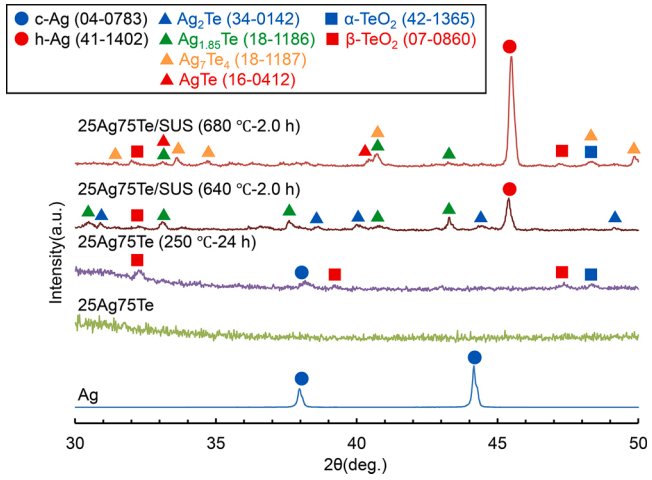

Fig. 8. XRD patterns of 25Ag75Te glass, heat-treated 25Ag75Te glass, 25Ag75Te/SUS, and reference Ag.

(640 ℃–2.0 h) was close to that of heat-treated 25Ag75Te (250 ℃–24 h) rather than that of 25Ag75Te/SUS (680 ℃–2.0 h). 25Ag75Te/SUS (680 ℃–2.0 h) precipitated hexagonal Ag, Ag_7Te_4, and AgTe along with α-TeO_2 and β-TeO_2. 25Ag75Te/SUS (680 ℃–2.0 h) had a very low pH sensitivity of ~5 %. When the samples were heat-treated at higher temperatures, the tendency that cubic Ag transforms to hexagonal Ag and Ag reacts with Te to produce Te rich AgTe alloys was observed. The hexagonal Ag as a principal phase and the only Ag_7Te_4 and AgTe with lower Ag/Te ratios along with α-TeO_2 and β-TeO_2 were observed in 25Ag75Te/SUS (680 ℃–2.0 h). The effect of TeO_2 on the pH sensitivity was neglected because they can have very high resistivity compared with Ag and Ag alloys and don't exist in conduction paths.

Ag_2O-TeO_2 glass, heat-treated Ag_2O-TeO_2 glass, and Ag_2O-TeO_2 glass/SUS differ in terms of electrode structure because the state of Ag on the glass surface depends on the heat treatment temperature. These electrodes were roughly categorized by the state of Ag on the glass surface as follows: (1) Ag_2O-TeO_2 glass: Ag^0-free, (2) Ag_2O-TeO_2 glass heat-treated at moderate temperature and Ag: cubic Ag^0 and (3) Ag_2O-TeO_2 glass/SUS heat-treated at high temperature: hexagonal Ag^0 and Ag alloys (Ag^0). Therefore, our results suggest that the crystal phase of Ag and alloying Ag and Te affect the pH sensitivity. A similar phenomenon is observed for the pH sensitivity of heat-treated stainless steel electrodes [7], although we have yet to identify the cause. The austenite phase (fcc) was the main phase on the surface of the heat-treated stainless steel electrodes. Unexpectedly, the change in the amount of martensite phase (bcc) of the second phase with the heat treatment temperature was similar to the pH sensitivity. Thus, these phenomena suggest that the phase transformation of metal can affect pH sensitivity. Hexagonal Ag and Ag alloys-precipitated glasses are candidate reference electrodes for pH sensors. It's hard to think that cubic and hexagonal Ag have largely different standard electrode potentials at present. We insist that standard electrode potentials of Ag-Te alloy with lower Ag/Te ratios, in which Te was incorporated to Ag at higher temperatures, come closer to zero than Ag by process of elimination. This investigation and the improvement of stability of potential due to chlorination are currently in progress.

4. Conclusions

In this study, new types of reference electrodes for pH sensors that are based on Ag and Ag alloys-precipitated Ag_2O-TeO_2 glass and Ag_2O-TeO_2 glass/stainless steel were developed.

- The pH sensitivity of Ag_2O-TeO_2 glasses increased as the Ag_2O content increased, but it was less than 40 % and the lowest among those of the glasses that have been investigated to date.
- The heat-treated $25Ag_2O \cdot 75TeO_2$ glass and $25Ag_2O \cdot 75TeO_2$ glass/stainless steel electrodes precipitated cubic Ag and hexagonal Ag and showed relatively low pH sensitivities of 26 % and 5 %, respectively. Thus, the hexagonal Ag and Ag alloys-precipitated samples were identified as candidate reference electrodes for pH sensors.

CRediT authorship contribution statement

Tadanori Hashimoto: Conceptualization, Methodology, Writing - original draft. **Keisuke Nakade:** Software, Investigation. **Atsushi Ishihara:** Supervision, Writing - review & editing. **Yuji Nishio:** Resources, Writing - review & editing.

Declaration of Competing Interest

The authors declare the following financial interests/personal relationships which may be considered as potential competing interests.

Acknowledgments

This work was supported by JSPS KAKENHI (JP18K04702). The authors thank Mr. Kazuki Naito, Mr. Kato Keiji, and Dr. Hiroyuki Nasu for their helpful work.

References

[1] Y. Nishio, T. Muroga, T. Hashimoto, A. Ishihara, Development of self-cleaning pH electrode coated with titanium oxide (TiO_2) and its photocatalytic activity, EICA 23 (2018) 69–74. http://eica.jp/search/paper_read.php?id=1477.

[2] T. Hashimoto, M. Wagu, K. Kimura, H. Nasu, A. Ishihara, Y. Nishio, Y. Iwamoto, Titanophosphate glasses as lithium-free nonsilicate pH-responsive glasses - compatibility between pH responsivity and self-cleaning properties, Mater. Res. Bull. 47 (2012) 1942–1949, https://doi.org/10.1016/j.materresbull.2012.04.030.

[3] T. Hashimoto, M. Hamajima, H. Ohta, H. Nasu, A. Ishihara, Y. Nishio, Fe_2O_3-Bi_2O_3-B_2O_3 glasses as lithium-free nonsilicate pH responsive glasses - compatibility between pH responsivity and hydrophobicity, Mater. Res. Bull. 50 (2014) 385–391, https://doi.org/10.1016/j.materresbull.2013.11.038.

[4] T. Hashimoto, F. Murayama, M. Nakao, H. Nasu, A. Ishihara, Y. Nishio, Drastic Dependence of the pH sensitivity of Fe_2O_3-Bi_2O_3-B_2O_3 hydrophobic glasses with composition, Materials 8 (2015) 8624–8629, https://doi.org/10.3390/ma8125480.

[5] T. Hashimoto, H. Inukai, K. Matsumura, H. Nasu, A. Ishihara, Y. Nishio, Effect of glass former (B_2O_3, SiO_2, GeO_2 and P_2O_5) addition to Fe_2O_3-Bi_2O_3 glass on pH responsivity, Sens. Actuators B Chem. 257 (2018) 807–814, https://doi.org/10.1016/j.snb.2017.11.053.

[6] T. Hashimoto, M. Miwa, H. Nasu, A. Ishihara, Y. Nishio, pH sensors using 3d-block metal oxide-coated stainless steel electrodes, Electrochim. Acta 220 (2016) 699–704, https://doi.org/10.1016/j.electacta.2016.10.166.

[7] T. Hashimoto, H. Kitabayashi, K. Ito, H. Nasu, A. Ishihara, Y. Nishio, Effect of heat-treatment on the pH sensitivity of stainless-steel electrodes as pH sensors, Heliyon 5 (2019), e01239, https://doi.org/10.1016/j.heliyon.2019.e01239.

[8] L. Manjakkal, D. Szwagierczak, R. Dahiya, Metal oxides based electrochemical pH sensors: current progress T and future perspectives, Prog. Mater. Sci. 109 (2020), 100635, https://doi.org/10.1016/j.pmatsci.2019.100635.

[9] R. Rahimi, M. Ochoa, T. Parupudi, X. Zhao, I.K. Yazdi, M.R. Dokmeci, A. Tamayol, A. Khademhosseini, B. Ziaie, A low-cost flexible pH sensor array for wound assessment, Sens. Actuators B Chem. 229 (2016) 609–617, https://doi.org/10.1016/j.snb.2015.12.082.

[10] Y. Qin, A.U. Alam, M.M.R. Howlader, N.X. Hu, M.J. Deen, Inkjet printing of a highly loaded palladium ink for integrated, low-cost pH sensors, Adv. Funct. Mater. 26 (2016) 4923–4933, https://doi.org/10.1002/adfm.201600657.

[11] W.J. Cho, C.M. Lim, Sensing properties of separative paper-based extended-gate ion-sensitive field-effect transistor for cost effective pH sensor applications, Solid State Electron. 140 (2018) 96–99, https://doi.org/10.1016/j.sse.2017.10.025.

[12] H. Kaden, H. Jahn, M. Berthold, Study of the glass/polypyrrole interface in an all-solid state pH sensor, Solid State Ion. 169 (2004) 129–133, https://doi.org/10.1016/S0167-2738(03)00216-9.

[13] W. Vonau, J. Gabel, H. Jahn, Potentiometric all solid state pH glass sensors, Electrochim. Acta 50 (2005) 4981–4987, https://doi.org/10.1016/j.electacta.2005.02.084.

[14] S. Nakayama, K. Onishi, T. Asahi, Y.L. Aung, S. Kuwata, Response characteristics of all-solid state pH sensor using $Li_5YSi_4O_{12}$ glass, Ceram. Intern. 35 (2009) 3057–3060, https://doi.org/10.1016/j.ceramint.2009.04.020.

[15] Q. An, S. Gan, J. Xu, Y. Bao, T. Wu, H. Kong, L. Zhong, Y. Mac, Z. Song, L. Niu, A multichannel electrochemical all-solid-state wearable potentiometric sensor for real-time sweat ion monitoring, Electrochem. Commun. 107 (2019), 106553, https://doi.org/10.1016/j.elecom.2019.106553.

[16] W. Lonsdale, S.P. Shylendra, M. Wajrak, K. Alameh, Application of all solid-state 3D printed pH sensor to beverage samples using matrix matched standard, Talanta 196 (2019) 18–21, https://doi.org/10.1016/j.talanta.2018.12.037.

[17] C. Zuliani, G. Matzeu, D. Diamond, A potentiometric disposable sensor strip for measuring pH in saliva, Electrochim. Acta 132 (2014) 292–296, https://doi.org/10.1016/j.electacta.2014.03.140.

[18] C. Hegarty, S. Kirkwood, M.F. Cardosi, C.L. Lawrence, C.M. Taylor, R.B. Smith, J. Davis, Disposable solid state pH sensor based on flavin polymer-ferrocyanide redox couples, Microchem. J. 139 (2018) 210–215, https://doi.org/10.1016/j.microc.2018.02.024.

[19] S.Z. Mohammadi, H. Beitollahi, H. Allahabadi, T. Rohani, Disposable electrochemical sensor based on modified screen printed electrode for sensitive cabergoline quantification, J. Electroanal. Chem. 847 (2019), 113223, https://doi.org/10.1016/j.jelechem.2019.113223.

[20] H.Y.Y. Nyein, W. Gao, Z. Shahpar, S. Emaminejad, S. Challa, K. Chen, H.M. Fahad, L.C. Tai, H. Ota, R.W. Davis, A. Javey, A wearable electrochemical platform for noninvasive simultaneous monitoring of Ca^{2+} and pH, ACS Nano 10 (2016) 7216–7224, https://doi.org/10.1021/acsnano.6b04005.

[21] M.A. Yokus, T. Songkakul, V.A. Pozdin, A. Bozkurt, M.A. Daniele, Wearable multiplexed biosensor system toward continuous monitoring of metabolites, Biosens. Bioelectron. 153 (2020), 112038, https://doi.org/10.1016/j.bios.2020.112038.

[22] M. Sophocleous, J.K. Atkinson, A review of screen-printed silver/silver chloride (Ag/AgCl) reference electrodes potentially suitable for environmental potentiometric sensors, Sens. Actuators A Phys. 267 (2017) 106–120, https://doi.org/10.1016/j.sna.2017.10.013.

[23] A. Lewenstam, B. Bartoszewicz, J. Migdalski, A. Kochan, Solid contact reference electrode with a PVC-based composite electroactive element fabricated by 3D printing, Electrochem. Commun. 109 (2019), 106613, https://doi.org/10.1016/j.elecom.2019.106613.

[24] A. Moya, R. Pol, A. Martínez-Cuadrado, R. Villa, G. Gabriel, M. Baeza, Stable full-inkjet-printed solid-state Ag/AgCl reference electrode, Anal. Chem. 91 (2019) 15539–15546, https://doi.org/10.1021/acs.analchem.9b03441.

[25] A. Bananezhad, M. Jović, L.F. Villalobos, K.V. Agrawal, M.R. Ganjali, H.H. Girault, Large-scale fabrication of flexible solid-state reference electrodes, J. Electroanal. Chem. 847 (2019), 113241, https://doi.org/10.1016/j.jelechem.2019.113241.

[26] H.R. Lim, N. Hillman, Y.T. Kwon, Y.S. Kim, Y.H. Cho, W.H. Yeo, Ultrathin, long-term stable, solid-state reference electrode enabled by enhanced interfacial adhesion and conformal coating of AgCl, Sens. Actuators B Chem. 309 (2020), 127761, https://doi.org/10.1016/j.snb.2020.127761.

[27] S. Lorant, C. Bohnke, M. Roffat, O. Bohnke, New concept of an all-solid state reference electrode using a film of lithium lanthanum titanium oxide (LLTO), Electrochim. Acta 80 (2012) 418–425, https://doi.org/10.1016/j.electacta.2012.07.051.

[28] V.M. Tolosa, K.M. Wassum, N.T. Maidment, H.G. Monbouquette, Electrochemically deposited iridium oxide reference electrode integrated with an electroenzymatic glutamate sensor on a multi-electrode array microprobe, Biosens. Bioelectron. 42 (2013) 256–260, https://doi.org/10.1016/j.bios.2012.10.061.

[29] S. Karthick, H.S. Lee, Y.S. Lee, J. Kumar Singh, S.J. Kwon, R. Natarajan, Fabrication of a cerium-doped nickel ferrite solid-state reference electrode and its performance evaluation in concrete environment, Sens. Actuators B Chem. 251 (2017) 509–523, https://doi.org/10.1016/j.snb.2017.05.002.

[30] W. Vonau, U. Guth, pH Monitoring: a review, J. Solid State Electrochem. 10 (2006) 746–752, https://doi.org/10.1007/s10008-006-0120-4.

[31] R. Zeng, J. Zhang, H. Yang, C. Sun, M. Xu, S.L. Zhang, D. Wu, Modelling and characterization of novel reference-less semiconductor ion T sensor for pH sensing, Sens. Actuators B. Chem. 281 (2019) 60–71, https://doi.org/10.1016/j.snb.2018.07.175.

[32] G. Parish, F.L.M. Khir, N.R. Krishnan, J. Wang, J.S. Krisjanto, H. Li, G.A. Umana-Membreno, S. Keller, U.K. Mishra, M.V. Baker, B.D. Nener, M. Myers, Role of GaN cap layer for reference electrode free AlGaN/GaN-based pH T sensors, Sens. Actuators B. Chem. 287 (2019) 250–257, https://doi.org/10.1016/j.snb.2019.02.039).

[33] D. Xue, H. Zhang, Au. Ahmad, H. Liang, J. Liu, X. Xia, W. Guo, H. Huang, N. Xu, Enhancing the sensitivity of the reference electrode free AlGaN/GaN HEMT based pH sensors by controlling the threshold voltage, Sens. Actuators B. Chem. 306 (2020), 127609, https://doi.org/10.1016/j.snb.2019.127609.

[34] D. Linda, M. Dutreilh-Colas, D. Hamani, P. Thomas, A. Mirgorodsky, J.-R. Ducle`re, O. Masson, M. Loukil, A. Kabadou, New glasses within the Tl_2O–Ag_2O–TeO_2 system: thermal characteristics, Raman spectra and structural properties, Mater. Res. Bull. 45 (2010) 1816–1824, https://doi.org/10.1016/j.snb.2008.12.001.

[35] K. Kato, T. Hayakawa, Y. Kasuya, P. Thomas, Influence of Al_2O_3 incorporation on the third-order nonlinear optical properties of Ag_2O–TeO_2 glasses, J. Non-Cryst. Solids 431 (2016) 97–102, https://doi.org/10.1016/j.jnoncrysol.2015.05.036.

[36] L. Pavic, A. Santic, J. Nikolic, P. Mosner, L. Koudelka, D. Pajic, A. Mogus-Milankovic, Nature of mixed electrical transport in Ag_2O-ZnO-P_2O_5 glasses containing WO_3 and MoO_3, Electrochim. Acta 276 (2018) 434–445, https://doi.org/10.1016/j.electacta.2018.04.029.

[37] A. Santic, J. Nikolic, L. Pavic, R.D. Banhatti, P. Mosner, L. Koudelka, A. Mogus-Milankovic, Scaling features of conductivity spectra reveal complexities in ionic, polaronic and mixed ionic-polaronic conduction in phosphate glasses, Acta Mater. 175 (2019) 46–54, https://doi.org/10.1016/j.actamat.2019.05.067.

[38] P. Cheng, Y. Zhou, X. Su, M. Zhou, Z. Zhou, The near-infrared band luminescence in silver NPs embedded tellurite glass doped with $Er^{3+}/Tm^{3+}/Yb^{3+}$ ions, J. Alloy Comp. 714 (2017) 370–380, https://doi.org/10.1016/j.jallcom.2017.04.067.
[39] P. Kurzweil, Metal oxides and ion-exchanging surfaces as pH sensors in liquids: state-of-the-art and outlook, Sensors 9 (2009) 4955–4985, https://doi.org/10.3390/s90604955.
[40] Cl. Bohnke, H. Duroy, J.L. Fourquet, pH sensors with lithium lanthanum titanate sensitive material: applications in food industry, Sens. Actuators B. Chem. 89 (2003) 240–247, https://doi.org/10.1016/S0925-4005(02)00473-2.
[41] F. Wang, J. Dai, L. Shi, X. Huang, C. Zhang, X. Li, L. Wang, Investigation of the melting characteristic, forming regularity and thermal behavior in lead-free V_2O_5–B_2O_3–TeO_2 low temperature sealing glass, Mater. Lett. 67 (2012) 196–198, https://doi.org/10.1016/j.matlet.2011.09.037.
[42] A. Marczewska, M. Środa, M. Nocuń, Thermal and spectroscopic characterization of gallium-tellurite glasses doped BaF_2 and PbO, J. Non-Cryst. Solids 464 (2017) 104–114, https://doi.org/10.1016/j.jnoncrysol.2017.03.026.
[43] C. Godoy, E.A. Souza, M.M. Lima, J.C.A. Batista, Correlation between residual stresses and adhesion of plasma sprayed coatings: effects of a post-annealing treatment, Thin Solid Films 420–421 (2002) 438–445, https://doi.org/10.1016/S0040-6090(02)00805-2.
[44] J. Rams, M. Campo, B. Torres, A. Ureña, Al/SiC composite coatings of steels by thermal spraying, Mater. Lett. 62 (2008) 2114–2117, https://doi.org/10.1016/j.matlet.2007.11.037.
[45] S. Søpstad, E.A. Johannessen, F. Seland, K. Imenes, Long-term stability of screen-printed pseudo-reference electrodes for electrochemical biosensors, Electrochim. Acta 287 (2018) 29–36, https://doi.org/10.1016/j.electacta.2018.08.045).
[46] G. Eisenman, Cation selective glass electrodes and their mode of operation, Biophys. J. 2 (1962) 259–323, https://doi.org/10.1016/S0006-3495(62)86959-8.
[47] J.L. Garvin, A simple method to determine millimolar concentrations of sodium in nanoliter samples, Kidney Int. 44 (1993) 875–880, https://doi.org/10.1038/ki.1993.325.
[48] A. Kumar, A. Singhal, Optical and magnetic behavior of Ag encapsulated β-Fe_2O_3 core–shell hollow nanotubes, Mater. Chem. Phys. 131 (2011) 230–240, https://doi.org/10.1016/j.matchemphys.2011.09.016.
[49] B. Tiana, W. Chen, D. Yu, Y. Lei, Q. Ke, Y. Guo, Z. Zhu, Fabrication of silver nanoparticle-doped hydroxyapatite coatings with oriented block arrays for enhancing bactericidal effect and osteoinductivity, J. Mech. Behav. Biomed. Mater. 61 (2016) 345–359, https://doi.org/10.1016/j.jmbbm.2016.04.002.

Tadanori Hashimoto is an associate professor in Mie University, Japan. He received his doctoral degree from Kyoto University, Japan in 1995. His current research interests include glass science, pH electrode and photocatalysis.

Keisuke Nakade received his bachelor's degree from Mie University, Japan in 2019. He joined in the master degree, Mie University, Japan in 2019-present. His current research interests include pH electrode.

Atsushi Ishihara is a professor in Mie University, Japan. He received his doctoral degree from Kyoto University, Japan in 1989. His current research interests include the generation of novel catalysis in petroleum, coal and biomass refining.

Yuji Nishio is a Manager in HORIBA Advanced Techno, Co., Ltd., Japan. He received his doctoral degree from Mie University, Japan in 2016. His current research interests include pH electrode and Chemical sensor.